# Finite element analysis of the effect of tibial prosthesis extension stem length in total knee arthroplasty in the Chinese population

**Yeran Li**
Jilin University First Hospital
**Yuhang Gao**
Jilin University First Hospital
**Lu Ding**
Jilin University First Hospital
**Chen Yang**
Jilin University First Hospital
**Jinlong Wang**
Jilin University First Hospital
**Xuebo Zhang**
Jilin University First Hospital
**Jianguo Liu**
Jilin University First Hospital
**Xin Qi** ( qixindoc@163.com )
The First Hospital of Jilin University, Jilin University, https://orcid.org/0000-0002-5280-6845

**Research article**

**Keywords:** Total knee arthroplasty, Tibial prosthesis, Extension stem, Finite element analysis, Posterior slope

**Posted Date:** December 19th, 2019

**DOI:** https://doi.org/10.21203/rs.2.19104/v1

# Abstract

## Background

This study aimed to determine the longest usable range of tibial prosthesis extension stems in Chinese patients undergoing primary total knee arthroplasty and to analyze the effect of different stem lengths on prosthesis stability within this range.

## Methods

We conducted three-dimensional modeling and simulated surgery in patients with genu varum to measure the longest usable range of tibial prothesis stems, identify impinged cortices under tibial posterior slope cut of 0° and 3°, and analyze factors influencing the longest stem length. We built finite element models according to the longest usable range of extension stems to simulate tibial prostheses with different stem lengths, measure the stress distribution of tibias and prostheses and the relative displacement of distal ends of prostheses, and investigate the effect of different stem extension lengths on prosthesis stability.

## Results

We simulated osteotomy with a tibial posterior slope cut of 0° and 3°, under which the maximum tibial prosthesis stem length was 83 mm (79±24 mm). The simulated tibial cut with a tibial posterior slope of 3° indicated the maximum tibial prosthesis stem length to be 83 mm (83±20 mm). According to the longest usable range of extension stems, we defined five groups for finite element analysis with 40-mm, 50-mm, 60-mm, 70-mm, and 80-mm stem lengths and analyzed each group for posterior slopes of 0° and 3°. The 80-mm stem length models showed minimum relative displacement of the distal end of tibial prosthesis (0°: 2.63, 1.61±0.05 μm; 3°: 1.48, 1.44±0.09 μm), whereas the 40-mm stem length models showed maximum relative displacement (0°: 3.16, 3.19±0.12 μm; 3°: 1.84, 1.81±0.07 μm). As the length of tibial prosthesis stems increased from 40 to 70 mm, the relative displacement of the distal end of prosthesis decreased for both posterior slopes but was insignificant when stem lengths increased to 70–80 mm.

## Conclusions

Based on the results, we suggest that using the longest tibial stem is not always necessarily a better option to increase stability, as the prosthesis shows greater stability in only a specific range of increased length but shows insignificant change when the length is greatly increased.

# Background

Primary total knee arthroplasty (TKA) provides good long-term outcomes with respect to pain relief and functional recovery in patients with knee osteoarthritis, rheumatoid arthritis (RA), and other knee degenerative diseases [1, 2]. The 10-year survival rate of primary TKA is reportedly 95.5–97.7% [3, 4, 5].

The most common cause of TKA failure is prosthesis loosening [6, 7], particularly on the tibial side [8, 9]. Some osteoporosis patients with severe varus deformities and poor soft tissue conditions due to RA are more likely to experience loosening of the tibial prostheses after primary TKA [10, 11, 12].

The purpose of this study was to determine the longest usable range of tibial prothesis extension stems in Chinese patients undergoing primary TKA and to analyze the effect of different stem lengths on prosthesis stability within this range.

# Methods

### Part 1: Construction of 3D tibial models under different stem lengths of tibial plateau

Patients suffering from osteoarthritis with genu varum (excluding those with suspected infection before surgery, previous knee surgery, or RA) were included in the study from May 2018 to May 2019. Full-length radiographs were preoperatively taken for both lower extremities, and the angle of varus deformity and the medial proximal tibial angle (MPTA) of the knees were measured. Subsequently, a 0.6-mm thin-slice CT scan of both lower extremities was conducted and Mimics 14.0 (Materialise, Leuven, Belgium) was used to construct a 3D model. A coordinate system was set up, with the z-axis as the tibial alignment line (i.e., the line connecting the center of ankle mortise and the center of any axial plane below the proximal tibial articular surface and above the tibial tuberosity). The tibial length along the direction of the force line was measured on the 3D model of the tibia. The y-axis was defined as the anteroposterior (AP) axis, which was determined by an experienced orthopedist (connecting the medial 1/3$^{rd}$ of the tibial tuberosity and the midpoint of posterior cruciate ligament endpoint in a plane perpendicular to the z-axis). The x-axis was a straight line perpendicular to the y-axis and z-axis. This model was simplified by ignoring the measurements of the fibula. Tibial cutting planes with posterior slopes of 0° and 3° were made to be perpendicular to the tibial force alignment line and were placed 8 mm away from the lateral side tibial plateau to simulate tibial cut. If no defect was found in the medial tibia after simulated tibial cut, the patient was enrolled as a subject. If the medial tibia had a defect less than 4 mm away from the tibial cutting plane, the osteotomy volume of the tibia was increased until the defect in the medial tibia was eliminated. If defect in the medial tibia was further away than 4 mm, the case was excluded from this study. A total of 100 samples were obtained using the above method.

From these 100 samples, appropriate tibial models were chosen. The model profiles were acquired from the directly measured results by press-fit condylar (PFC) Sigma (Depuy Orthopaedics, Warsaw, IN, USA) and were assembled according to the manufacturer's guidelines. The rotation of the tibial prothesis was consistent with the y-axis direction in the coordinate system (i.e., the AP axis of the tibia). The maximum length of the tibial prothesis stem that could be inserted and the distal end of the stem that impinged the tibial cortex when the tibial prosthesis was in the proper position were measured for the two groups undergoing tibial cut with different tibial posterior slopes (0° and 3°), as shown in Fig. 1.

## Part 2: Establishment of finite element models to show the effect of different lengths of tibial plateau extension stems on the stress distribution of tibial prosthesis

### Basic model

A 3D model with the tibial length equivalent to the median of the tibial length measured in Part 1 was chosen. Mimics software was used to establish models for the cortical and cancellous bones, and a coordinate system and alignment line were established, as described in Part 1. The models were simplified by ignoring the fibular measurements. Tibial cuts with tibial posterior slopes of 0° and 3° were simulated using the same tibial cut method, as described in Part 1. The basic models were obtained after checking their integrity following simulated tibial cut.

### Tibial components

To determine the tibial components, an appropriate tibial plateau model was selected, and the model profile was obtained by direct measurement according to the PFC Sigma (DePuy Orthopaedics, Warsaw, IN, USA) and the model was assembled according to the manufacturer's instructions. The rotation of tibial prothesis was consistent with the y-axis in the Part 1 method (i.e., the AP axis of the tibia). According to the confidence interval (CI) of the maximum stem length measured in Part 1, tibial plateau models with different stem lengths for prosthesis were set up. An 8-mm tibial spacer was selected. As knee motion was not considered during the modeling, the upper contour of the spacer was omitted and replaced by a plateau [15, 16]. Under the plateau, the thickness of bone cement was simulated as a 1-mm rigid body, which is in line with previous studies [17, 18, 19, 20].

### Finite element models of tibia prostheses with different extension stem lengths

Two groups undergoing tibial cut with tibial posterior slopes of 0° and 3° were established as described in Part 1, with each group having five different extension stem lengths according to the CI of maximum range stem length measured in Part 1. They constituted a total of ten models with different extension stem lengths for tibial plateau prostheses and two posterior slopes. The models of tibial plateaus and spacers were installed, after which HyperMesh (Altair HyperWorks, Troy, MI, USA) was used for finite element meshing. The finite element models are shown in Fig. 2.

### Material properties

Based on previous research data, the densities, Poisson's ratios, and elastic moduli of the tibial cortical bone, cancellous bone, plateau, placers, sclerotic bone, and bone cement were defined, as shown in Table 1 [16, 17, 21, 22, 23]. The coefficients of friction were measured: between the tibia and bone cement = 1, between the bone cement and tibial plateau = 0.4, and between other contact surfaces = 0.4 [17, 18, 19, 20].

### Load and boundary conditions

The inferior surface of the distal tibia was fixed in all directions. The maximum load and the medial and lateral distributions were similar to those described in previous studies. Static standing with exact mechanical alignment was simulated with 50% load on medial side and 50% on the lateral side of the spacer [24]. The force was set at three times the total body weight (e.g., total body weight 70 kg = 2100 N). The force-bearing site was the transverse diameter of the tibial prosthesis across the medial and lateral plateau center [15, 17, 21, 25]. The direction of the force was parallel to the tibial alignment (z-axis). The relative displacement of distal end of the prothesis and the stress distribution among the prosthesis and tibia were compared [16].

### Statistical analysis

All data were expressed as mean ± standard deviation. Pearson's correlation coefficient was provided to assess the extent of linear association in the 0° and 3° groups. Statistical significance was defined as $p<0.1$. Statistical analyses were performed using Statistical Package for the Social Sciences version 17.0 (SPSS, Chicago, IL, USA).

## Results

In these selected cases, the tibial length was 334 mm (333±28 mm) with a 95% CI of 324–341 mm. The tibial length satisfied normal distribution with $p=0.215$. Approximately 46% of these patients were implanted with No. 2.5 tibial plateau prosthesis, 22% with No. 3 prosthesis, 12% with No. 2 prosthesis, 8% with No. 1.5 prosthesis, 6% with No. 4 prosthesis, and 6% with No. 5 prosthesis.

Under tibial cut with a tibial posterior slope of 0°, when the tibial plateau prosthesis was installed to simulate the surgery, the maximum stem length was 83 mm (79±24 mm), and the 95% CI was 72–86 mm, which satisfied normal distribution with $p=0.8$. When the MPTA was too large (>83°), the tibial plateau extension stem mostly impinged the cortical bone from the posterolateral tibial prothesis. When the MPTA was too small (<83°), the tibial stem penetrated the cortical bone from the posteromedial tibial prothesis. After excluding the effect of MPTA and simulating tibial cut with a tibial posterior slope of 0°, the extent of longest penetration by the prosthesis was related to the tibial length ($r=-0.412$, $p=0.013$). Regression analysis was conducted to determine the tibial length and maximum stem length of tibial plateau prosthesis, and the following equation was obtained for the Chinese population with 0° tibial cut:

*Maximum stem length of tibial prosthesis = 0.306 * tibial length - 22.477*

Based on this regression equation and the 95% CI (324–341 mm) of tibial length, we deduced that the maximum stem length for the Chinese population undergoing osteotomy with a tibial posterior slope of 0° was **77–83 mm**.

For those undergoing tibial cut with a tibial posterior slope of 3°, when the tibial plateau prosthesis was installed to simulate the surgery, the maximum stem length was 83 mm (83±20 mm) and the 95% CI was 72–86 mm, which satisfied normal distribution with $p=0.14$. The extension stem mostly penetrated the

cortical bone from the anteromedial tibia, without correlation with MPTA ($p>0.05$). In addition, the tibial length and preoperative varus angle had little influence on the penetrating position ($p>0.05$).

Finite element models were established by applying the median of tibial length and most commonly used type of tibial plateau prosthesis to simulate TKA with different stem lengths.

The length of a conventional base model of tibial prosthesis is 40 mm and the maximum length measured by us was 80 mm. Different stem length models were established as 40 mm, 50 mm, 60 mm, 70 mm, and 80 mm.

Fig. 3 shows the stress distribution of tibial plateau prosthesis. As the stem length of tibial plateau prosthesis increased, the stress in the stem region of the prosthesis and the stress concentration regions increased gradually in both groups with tibial posterior slopes of 0° and 3°.

Fig. 4 shows the stress distribution on the tibia under the tibial plateau prosthesis after TKA. With the increasing length of extension stem, the stress concentration appeared at the proximal end of the tibia under the tibial plateau prosthesis in both osteotomy groups with tibial posterior slopes of 0° and 3°, and the tibial stress under the tibial plateau prosthesis was reduced with the increasing length of the extension stem.

Fig. 5 shows the relative displacement of the most distal end of the tibial prosthesis compared with various stem lengths. Under osteotomy with tibial posterior slopes of 0° and 3°, the stem length of the tibial plateau prosthesis was in the range of 40–80 mm. With increasing stem lengths in the range of 40–70 mm, the relative displacement of the most distal end of the tibial plateau prosthesis decreased gradually (tibial posterior slope of 0°: 40 mm: 3.16, 3.19±0.12 μm, 50 mm: 2.99, 3.0±0.17 μm, 60 mm: 2.85, 2.87±0.1 μm; tibial posterior slope of 3°: 40 mm: 1.84, 1.81±0.07 μm, 50 mm: 1.74, 1.8±0.1, 60 mm: 1.6, 1.54±0.1 μm). When the stem length of the tibial plateau prosthesis reached 70–80 mm, the relative displacement of the distal end of tibial plateau prosthesis under both tibial posterior slopes varied slightly (tibial posterior slope of 0°: 0 mm: 2.66, 2.64±0.05 μm, 80 mm: 2.63, 1.61±0.05 μm) (tibial posterior slope of 3°: 70 mm: 1.52, 1.47±0.08, 80 mm: 1.48, 1.44±0.09 μm). The changing pattern is shown in Fig. 5.

# Discussion

To the best of our knowledge, this is the first study to investigate the maximum usable extension stem length of tibial plateau prosthesis, as well as the cortical impingement of the longest stem in the Chinese population. Based on the selected cases, 3D models were built to simulate surgery and measure relevant parameters. The regression equation of tibial length and the maximum stem length of tibial plateau prosthesis for the Chinese population was obtained by statistical analysis. This equation makes convenient to estimate the maximum usable stem length of tibial plateau prosthesis in TKA, and further guides the choice of extension stems for tibial plateau prostheses.

According to our study, for primary TKA, the stem length of tibial plateau prosthesis significantly influenced prosthesis stability irrespective of a tibial posterior slope of 0° or 3°. According to our measurement , as the longest measured stem length suitable for Chinese patients was 77–83 mm, we set up experimental groups with a stem length of up to 80 mm. When the stem length of the tibial plateau prosthesis was in the range of 40–70 mm, the prosthesis was more stable with the longer stem length. However, even when the stem length reached a higher measurement range of 70–80 mm, the influence of stem length on prosthesis stability tended to be similar. Previous studies have reported that using the tibial extension stem indeed improved prosthesis stability during primary TKA [10, 11, 13, 14]; however, these studies only compared the stability of tibial prosthesis between cases in which the extension stems were used and cases in which they were not used. They also lacked an accurate analysis of the effects of different stem lengths on the stability of tibial prostheses. Walsh *et al.* [11] carried out biomechanical experiments through *in vitro* models and found that the relative displacement of tibial prosthesis was smaller when using an extension stem compared to not using an extension stem (5–10 mm vs 10–20 mm), which is similar to the measurement results of our finite element models (2.4 mm vs 3.2 mm) using proximate numbers. With respect to the differences, we believe that Walsh *et al.* applied sawbones to perform the simulation, the properties of which are quite different from those of real bones, whereas our data more closely reflected real bone tissues [11]. Their study showed that tibial prostheses with stem lengths of 75 mm and 150 mm in the revision surgery had almost the same stability. Although their study was not conducted based on primary TKA, we obtained results similar to theirs—that is, tibial prostheses with stem lengths of over 70 mm achieved similar stability. Jan *et al.* applied various types of extension stems in knee revision surgery, but they only focused on bone stress around the prosthesis and did not investigate prosthesis stability [26]. They found that extension stems showed areas of stress concentration, which is consistent with our conclusions. We observed that stress concentration areas appear around the extension stem and disperse the bone stress of the tibia, which effectively explains why extension stems enhance prosthesis stability.

Our study had some limitations. First, we concluded all results based on static models and did not perform dynamic analyses. However, it has been previously reported that peak stress in knees occurs while standing, shortly before performing contralateral heel-down. Therefore, our study could also simulate a situation in which the prosthesis is subjected to peak stress [21]. Second, the effect of soft tissues on the prosthesis was not considered in our models. As studies similar to ours did not also consider the effect of soft tissues [15, 16, 25], we primarily focused on the static knee prosthesis and tibial sclerotic bone, the elastic moduli of which are significantly larger than that of soft tissues. Therefore, our simulation still holds practical significance. Third, we only targeted the Chinese population and our sample size was relatively small. In the future, multicenter studies are required to confirm the results of our study.

# Conclusions

In TKA, tibial cut with a tibial posterior slope of either 0° or 3° showed the stem length of the tibial plateau prosthesis having a significant positive influence on the stability of the tibial prosthesis. Using a stem

measuring 40–70 mm led to the tibial plateau prosthesis showing greater stability; however, using a stem measuring 70–80 mm showed that the increase in stem length showed almost no change in its influence on prosthesis stability. This suggested that using an extension with a longer length is not always beneficial, as the stability appears to remain sustained in a range of lengths and remains the same even when the stem becomes too long. These findings held true for the Chinese population, but future studies that are conducted across multiple centers and populations may reveal interesting results that will add to our knowledge.

# Abbreviations

**AP:** Anteroposterior

**CI:** Confidence interval

**MPTA:** Medial proximal tibial angle

**PFC:** Press-fit condylar

**RA:** Rheumatoid arthritis

**TKA:** Total knee arthroplasty

# Declarations

### Ethics approval and consent to participate:

This article contains a study with human participants, and the study protocol was approved by the Ethics Committee of the First Hospital of Jilin University (IRB #NA_00008484). Informed consent for this study was obtained from all patients by both written and verbal.

### Consent for publication:

Applicable. Written informed consent was obtained from the patient's guardian/parent/next of kin for the publication of this report and any accompanying images.

### Availability of data and materials:

The datasets generated and/or analysed during the current study are not publicly available due to individual privacy but are available from the corresponding author on reasonable request.

### Competing interests:

The authors declare that they have no competing interests.

### Funding

This study was funded by the Natural Science Funding of Jilin Province (grant number: 11 20170414020GH) and Health Technology Innovation Project of Jilin Province (grant number: 2018J057).

### Authors' contributions

XQ and JGL participated in the design of this study. YRL, CY, and YHG conducted the studies and performed the statistical analysis. YRL, LD, JLW, and XBZ drafted the manuscript. All authors read and approved the final manuscript.

### Acknowledgements

We extend sincere gratitude to the staff of the Department of Orthopaedic Surgery for their assistance during this study.

## References

1. Argenson JN, Boisgard S, Parratte S, Descamps S, Bercovy M, Bonnevialle P, et al. Survival analysis of total knee arthroplasty at a minimum 10 years' follow-up: a multicenter French nationwide study including 846 cases. Orthop Traumatol Surg Res. 2013;99:385-90. doi:10.1016/j.otsr.2013.03.014.
2. Gøthesen O, Espehaug B, Havelin L, Petursson G, Lygre S, Ellison P, et al. Survival rates and causes of revision in cemented primary total knee replacement. Bone Joint J. 2013;95:636-42. doi:10.1302/0301-620X.95B5.
3. Feng B, Weng X, Lin J, Jin J, Wang W, Qiu G. Long-term follow-up of cemented fixed-bearing total knee arthroplasty in a Chinese population: a survival analysis of more than 10 years. J Arthroplasty. 2013;28:1701-6. doi:10.1016/j.arth.2013.03.009.
4. Meftah M, Ranawat AS, Ranawat CS. Ten-year follow-up of a rotating-platform, posterior-stabilized total knee arthroplasty. J Bone Joint Surg Am. 2012;94:426-32. doi:10.2106/JBJS.K.00152.
5. De Martino I, D'Apolito R, Sculco PK, Poultsides LA, Gasparini G. Total knee arthroplasty using cementless porous tantalum monoblock tibial component: a minimum 10-year follow-up. J Arthroplasty. 2016;31:2193-8. doi:10.1016/j.arth.2016.03.057.
6. Sharkey PF, Lichstein PM, Shen C, Tokarski AT, Parvizi J. Why are total knee arthroplasties failing today–has anything changed after 10 years? J Arthroplasty. 2014;29:1774-8. doi:10.1016/j.arth.2013.07.024.
7. Schroer WC, Berend KR, Lombardi AV, Barnes CL, Bolognesi MP, Berend ME, et al. Why are total knees failing today? Etiology of total knee revision in 2010 and 2011. J Arthroplasty. 2013;28:116-9. doi:10.1016/j.arth.2013.04.056.
8. Keating EM, Meding JB, Faris PM, Ritter MA. Long-term followup of nonmodular total knee replacements. Clin Orthop Relat Res. 2002;34-9. doi:10.1097/00003086-200211000-00007.
9. Berend ME, Ritter MA, Meding JB, Faris PM, Keating EM, Redelman R, et al. Tibial component failure mechanisms in total knee arthroplasty. Clin Orthop Relat Res. 2004;26-34.

doi:10.1097/01.blo.0000148578.22729.0e.

10. Hamai S, Miyahara H, Esaki Y, Hirata G, Terada K, Kobara N, et al. Mid-term clinical results of primary total knee arthroplasty using metal block augmentation and stem extension in patients with rheumatoid arthritis. BMC Musculoskelet Disord. 2015;16:225. doi:10.1186/s12891-015-0689-9.
11. Walsh CP, Han S, Canham CD, Gonzalez JL, Noble P, Incavo SJ. Total knee arthroplasty in the osteoporotic tibia: a biomechanical evaluation of the role of stem extensions and cementing techniques. J Am Acad Orthop Surg. 2019;27:370-4. doi:10.5435/JAAOS-D-17-00736.
12. Ritter MA, Davis KE, Davis P, Farris A, Malinzak RA, Berend ME, et al. Preoperative malalignment increases risk of failure after total knee arthroplasty. J Bone Joint Surg Am. 2013;95:126-31. doi:10.2106/JBJS.K.00607.
13. Meijer MF, Boerboom AL, Stevens M, Reininga IHF, Janssen DW, Verdonschot N, et al. Tibial component with and without stem extension in a trabecular metal cone construct. Knee Surg Sports Traumatol Arthrosc. 2017;25:3644-52. doi:10.1007/s00167-016-4271-2.
14. Prudhon JL, Verdier R, Caton JH. Primary cementless total knee arthroplasty with or without stem extension: a matched comparative study of ninety eight standard stems versus ninety eight long stems after more than ten years of follow-up. Int Orthop. 2019;43:1849-57. doi:10.1007/s00264-018-4191-5.
15. Chong DY, Hansen UN, Amis AA. Analysis of bone-prosthesis interface micromotion for cementless tibial prosthesis fixation and the influence of loading conditions. J Biomech. 2010;43:1074-80. doi:10.1016/j.jbiomech.2009.12.006.
16. Totoribe K, Chosa E, Yamako G, Hamada H, Ouchi K, Yamashita S, et al. Finite element analysis of the tibial bone graft in cementless total knee arthroplasty. J Orthop Surg Res. 2018;13:113. doi:10.1186/s13018-018-0830-1.
17. Kang K, Jang YW, Yoo OS, Jung D, Lee SJ, Lee MC, et al. Biomechanical characteristics of three baseplate rotational arrangement techniques in total knee arthroplasty. Biomed Res Int. 2018;2018:9641417. doi:10.1155/2018/9641417.
18. Kang KT, Kwon SK, Kwon OR, Lee JS, Koh YG. Comparison of the biomechanical effect of posterior condylar offset and kinematics between posterior cruciate-retaining and posterior-stabilized total knee arthroplasty. Knee. 2019;26:250-7. doi:10.1016/j.knee.2018.11.017.
19. Kang KT, Koh YG, Son J, Kwon OR, Lee JS, Kwon SK. Comparison of kinematics in cruciate retaining and posterior stabilized for fixed and rotating platform mobile-bearing total knee arthroplasty with respect to different posterior tibial slope. Biomed Res Int. 2018;2018:5139074. doi:10.1155/2018/5139074.
20. Perillo-Marcone A, Taylor M. Effect of varus/valgus malalignment on bone strains in the proximal tibia after TKR: an explicit finite element study. J Biomech Eng. 2007;129:1-11. doi:10.1115/1.2401177.
21. Halder A, Kutzner I, Graichen F, Heinlein B, Beier A, Bergmann G. Influence of limb alignment on mediolateral loading in total knee replacement: in vivo measurements in five patients. J Bone Joint

Surg Am. 2012;94:1023-9. doi:10.2106/jbjs.K.00927.

22. Zysset PK, Sonny M, Hayes WC. Morphology-mechanical property relations in trabecular bone of the osteoarthritic proximal tibia. J Arthroplasty. 1994;9:203-16. doi:10.1016/0883-5403(94)90070-1.
23. Peters AE, Akhtar R, Comerford EJ, Bates KT. Tissue material properties and computational modelling of the human tibiofemoral joint: a critical review. PeerJ. 2018;6:e4298. doi:10.7717/peerj.4298.
24. Miller EJ, Riemer RF, Haut Donahue TL, Kaufman KR. Experimental validation of a tibiofemoral model for analyzing joint force distribution. J Biomech. 2009;42:1355-9. doi:10.1016/j.jbiomech.2009.03.019.
25. Innocenti B, Truyens E, Labey L, Wong P, Victor J, Bellemans J. Can medio-lateral baseplate position and load sharing induce asymptomatic local bone resorption of the proximal tibia? A finite element study. J Orthop Surg Res. 2009;4:26. doi:10.1186/1749-799X-4-26.
26. Quilez MP, Seral B, Pérez MA. Biomechanical evaluation of tibial bone adaptation after revision total knee arthroplasty: a comparison of different implant systems. PLoS One. 2017;12:e0184361. doi:10.1371/journal.pone.0184361.

# Table

**Table 1 Properties of materials used in the finite element model**

| Parts of the finite element model | Elastic modulus (GPa) | Material property (Poisson's ratio) | Density (g/cm³) |
|---|---|---|---|
| Cortical bone | 17 | 0.36 | 1.64 |
| Cancellous bone | 0.3 | 0.3 | 0.27 |
| Tibial component (baseplate) | 200 | 0.33 | 8 |
| Tibial component (spacer) | 0.9 | 0.46 | 0.94 |
| Bone cement | 2.3 | 0.3 | 1.19 |

# Figures

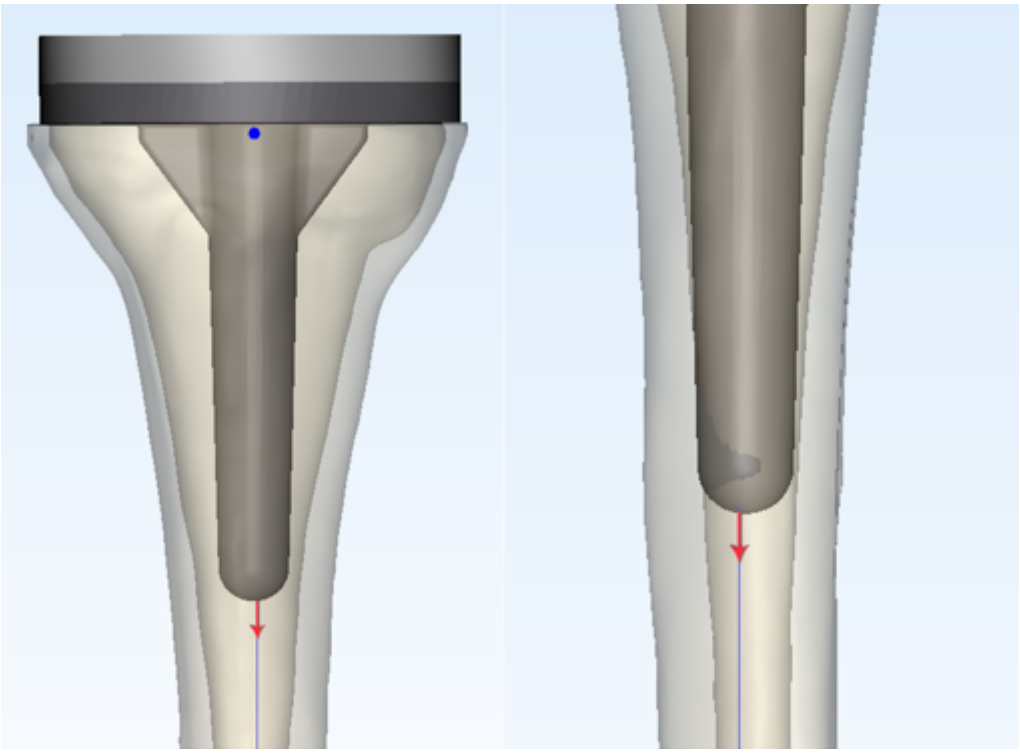

**Figure 1**

Evaluation of the maximum length of the tibial prothesis stem that could be inserted and the distal end of the stem that impinged the tibial cortex when the tibial prosthesis was in the proper position. The red arrow and blue line indicate tibial alignment

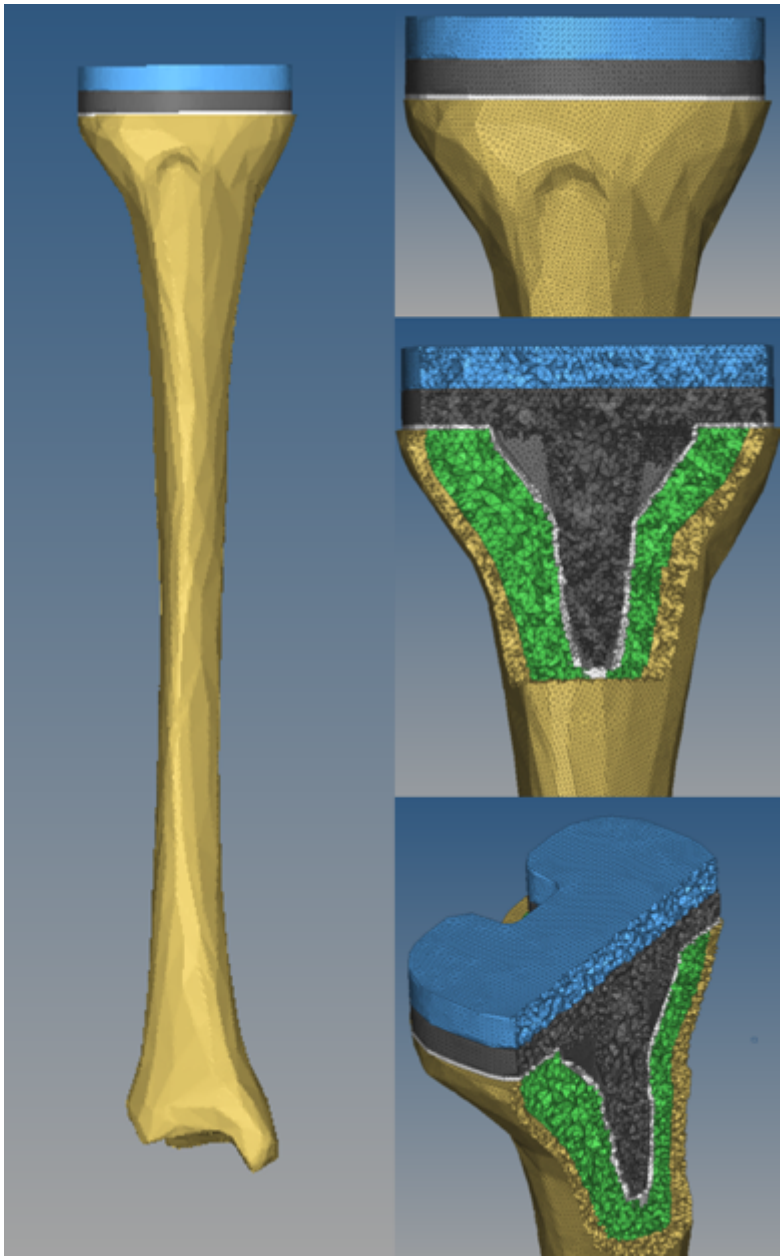

## Figure 2

An example of finite element analysis of the 60-mm tibial extension stem model

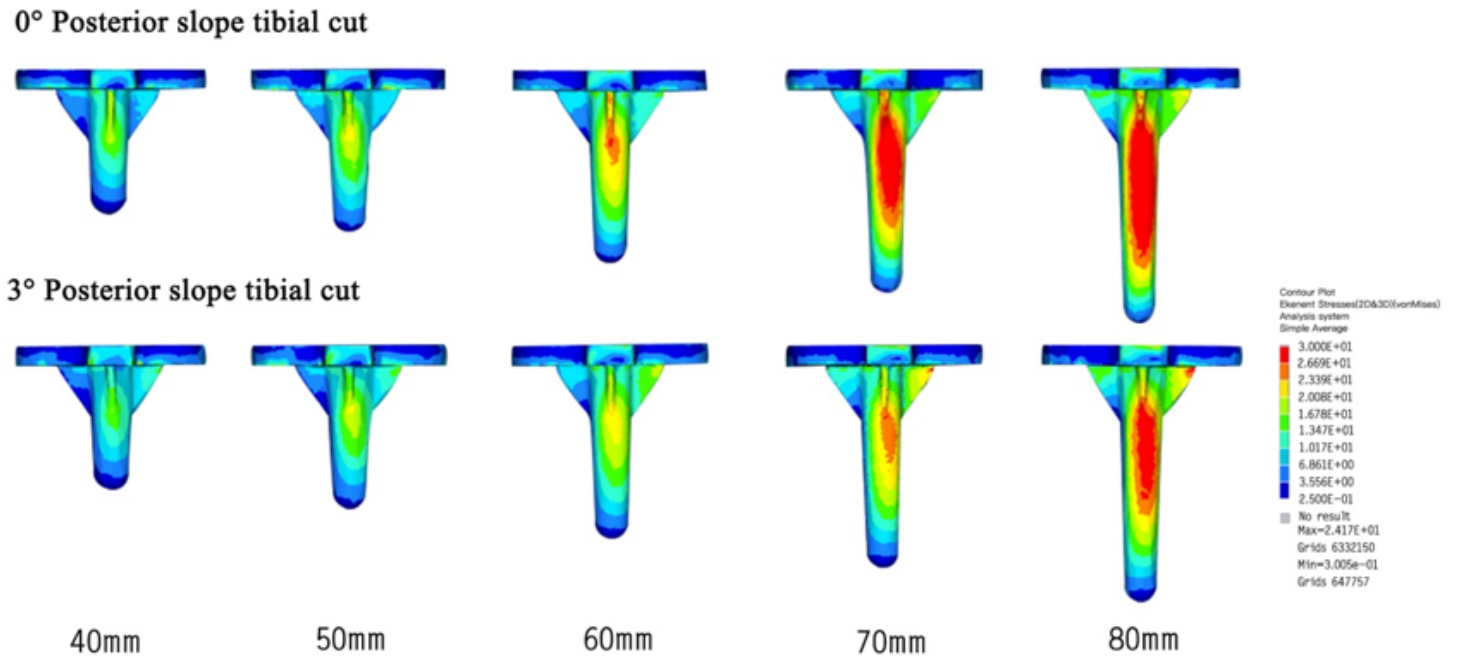


## Figure 3

Stress distribution of tibial plateau prosthesis. As the stem length of tibial plateau prosthesis increased, the stress in the stem region of the prosthesis and the stress concentration regions increased gradually in both osteotomy groups, with tibial posterior slopes measuring 0° and 3°, respectively

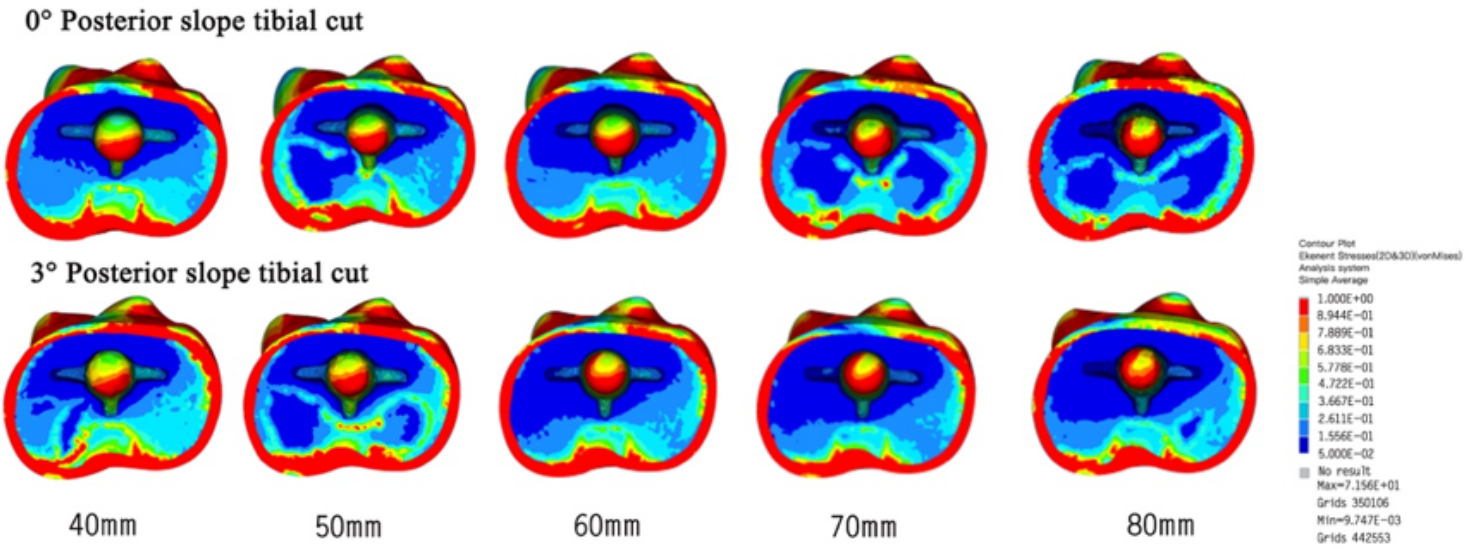


## Figure 4

Stress distribution on the tibia under the tibial plateau prosthesis after total knee arthroplasty

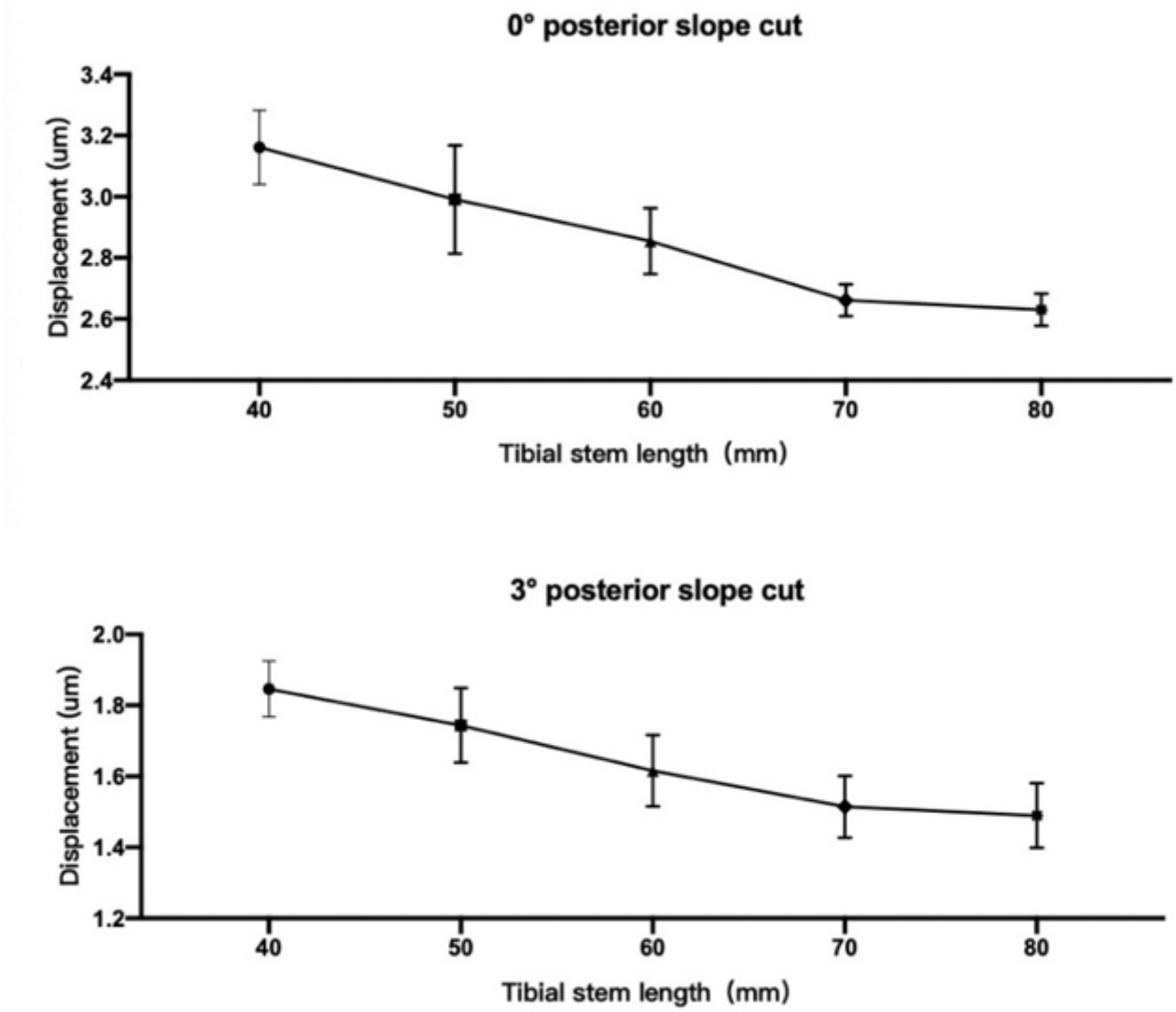


## Figure 5

Comparison of relative displacement of the most distal end of tibial prosthesis with various stem lengths